nature geoscience

LETTERS

PUBLISHED ONLINE: 8 JUNE 2015 | DOI: 10.1038/NGEO2456

Steeper temporal distribution of rain intensity at higher temperatures within Australian storms

Conrad Wasko and Ashish Sharma*

The mechanisms that cause changes in precipitation, as well as the resulting storm dynamics, under potential future warming remain debated[1–3]. Measured sensitivities of precipitation to temperature variations in the present climate have been used to constrain model predictions[4,5], debate precipitation mechanisms[2,3] and speculate on future changes to precipitation[6] and flooding[7]. Here, we analyse data sets of precipitation measurements at 6-min resolution from 79 locations throughout Australia, covering a broad range of climate zones, along with sub-daily temperature measurements of varying resolution. We investigate the relationship between temporal patterns of precipitation intensity within storm bursts and temperature variations in the present climate by calculating the scaling of the precipitation fractions within each storm burst. We find that in the present climate, a less uniform temporal pattern of precipitation—more intense peak precipitation and weaker precipitation during less intense times—is found at higher temperatures, regardless of the climatic region and season. We suggest invigorating storm dynamics could be associated with the warming temperatures expected over the course of the twenty-first century, which could lead to increases in the magnitude and frequency of short-duration floods.

There is considerable evidence that heavy precipitation events are increasing in frequency and intensity[8–10]. However, as the current generation of general circulation models (GCMs) are not a reliable predictor of precipitation extremes, the sensitivity of precipitation to temperature in historical records forms the basis of constraining GCM predictions[4], speculating on future changes to precipitation[6] and flooding[7], and debating dominant precipitation mechanisms[2,3]. This is because, in the absence of changes in humidity and large-scale circulation patterns, as per the Clausius–Clapeyron relationship, the atmosphere contains more moisture at warmer temperatures, resulting in heavier precipitation[11]. The observed relationship of precipitation with temperature from natural variability in the present climate is termed 'scaling'. Scaling depends heavily on the study location[12–14], the precipitation type[2], and the temperature range[7,13]. Owing to observed and modelled scaling being greater than what the Clausius–Clapeyron relationship predicts[5,15–17] debate remains on the interpretation of the results from these relationships and mechanisms causing intense rainfall bursts[1,2].

As the magnitude of the scaling decreases with increasing storm duration[12,18], this suggests changes occur to the precipitation intensity within storm bursts. Previous studies have considered only fixed durations when investigating the relationship between precipitation intensity and temperature, and have not looked at changes that may be happening within the storm burst. We hypothesize that at higher temperatures in the present climate, independent of the average precipitation intensity within the storm, a precipitation event may have an increase in its peak precipitation intensity with a simultaneous decrease in the non-peak precipitation segments (Fig. 1a). We first investigate whether the overall storm burst intensity, termed storm volume, scales with temperature, and subsequently look at the scaling of individual fractions of the storm burst, termed the temporal pattern, to see if the scaling in the temporal pattern dominates changes to the storm intensity.

Measurements of sub-daily precipitation of 6-min resolution and near-surface dry-bulb temperature across Australia were used. The Australian continent covers a large range of expected scaling of precipitation with temperature[12,13]. At each weather station, for a given storm burst duration, the largest 500 storm bursts in volume were chosen. Each storm burst was matched to its coincident temperature. Several different storm burst durations were chosen, ranging from one hour to twelve hours, with the precipitation record accumulated such that each storm burst consisted of five equal duration periods. For example, if a 1-h storm burst was analysed, the precipitation was accumulated to consist of five 12-min periods. Likewise a 2-h storm burst consisted of five 24-min increments, and a 3-h storm burst consisted of five 36-min increments. The storm burst volume (V) is defined as the total depth (in mm) for a given storm burst duration. Temporal patterns were constructed by dividing the storm burst by its volume. The individual precipitation fractions within the temporal pattern were assigned a rank (i), from largest to smallest, with the largest precipitation fraction being assigned a rank of 1 and the smallest assigned a rank of 5 (Fig. 1a).

The scaling of the hourly storm burst volume (α_V) at each station is presented in Supplementary Fig. 1. The regression lines fitted to the data at Sydney are presented in Supplementary Fig. 3. The majority of the sites showed a statistically significant positive scaling in the storm volume of 1% per °C to 5% per °C, with a median of the order of 2% per °C. Similar to previous studies, there is some evidence of a negative scaling in the storm volume at the northern latitudes[12–14].

Each hourly storm burst was subsequently split into five periods, each of which was 12 min in length. Figure 1b presents the scaling with temperature for the highest precipitation fraction, corresponding to the first rank (α_1). The majority of the sites exhibit a positive scaling with temperature ($\alpha_1 > 0$). The exceptions to this include two sites on the west coast of Australia, three sites on the southern mainland and one site in the northeast of the mainland. However, the results from only one of these sites was statistically significant. In general, almost all of the sites show a statistically significant positive scaling in the largest precipitation fraction of approximately 1–3% per °C, with a median increase of 2.1% per °C. This suggests that for hourly precipitation events, in addition to the storm volume scaling, the proportion of precipitation responsible for the flood peak scales at 2.1% per °C.

Figure 1c shows the results for the smallest precipitation fraction, the precipitation that corresponds to the fifth rank. In contrast to the above results, a statistically significant negative scaling ($\alpha_5 < 0$) at almost all of the sites was found. The magnitude of this scaling

School of Civil and Environmental Engineering, University of New South Wales, Sydney, New South Wales 2052, Australia. *e-mail: a.sharma@unsw.edu.au

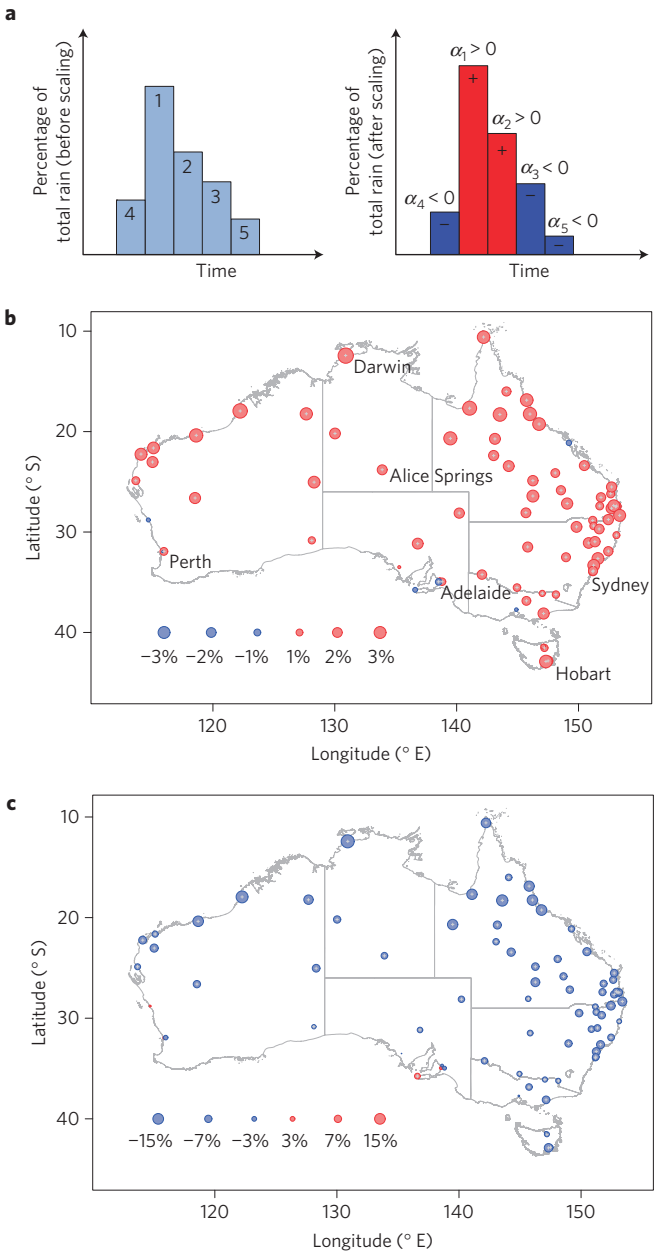

Figure 1 | Scaling of hourly storm burst temporal pattern. a, Schematic of temporal pattern scaling. The storm burst is divided into five equal periods and the precipitation fractions are ranked from largest to smallest. The two largest fractions scale positively, whereas the smallest three fractions scale negatively, resulting in a less uniform temporal pattern. **b**, Measured scaling for the largest precipitation fraction (α_1). **c**, Measured scaling for the smallest precipitation fraction (α_5). Crosses indicate statistical significance at the 95% confidence level testing against the null hypothesis that the slope of the regression line is zero. The circle area is proportional to scaling.

is larger than the increase for the first fraction, generally ranging from −3 to −15% per °C with a median value of −6.4% per °C. The sites that did not scale negatively are generally the same sites that did not scale positively for the highest precipitation fraction. The negative scaling of 6.4% per °C is actually greater in magnitude than the positive scaling in storm volume, indicating that, in absolute terms, the smallest precipitation amount within the storm is actually scaling negatively even though the entire storm volume is scaling positively. Consistent results were found when the data was stratified on whether the storm burst precipitation was predominately stratiform or convective (Supplementary Figs 7 and 8) or summer or winter dominant (Supplementary Figs 10 and 11).

Table 1 | Scaling (% per °C) of all precipitation fractions for a 60-min storm duration with five periods.

Location (station number)	Rank (*i*)				
	1	2	3	4	5
Perth (009021)	1.3	−0.1	−2.0	−2.6	−2.7
Darwin (014015)	4.9	2.2	−1.8	−12.4	−22.4
Alice Springs (015590)	2.1	0.9	−2.6	−4.9	−5.9
Adelaide (023090)	0.4	0.3	−1.5	−1.5	−0.9
Sydney (066062)	1.7	0.1	−1.7	−4.2	−6.1
Hobart (094029)	3.3	0.6	−3.6	−5.8	−9.4

This analysis was repeated for the intermediate ranks (2–4) for a range of selected sites, and a transition in the scaling from the highest fraction to the lowest fraction was observed. The first fraction had the largest positive scaling with temperature, whereas the fifth rank fraction had the largest negative scaling with temperature (see Table 1). The scaling for the intermediate fractions decreased with increasing rank. All the temporal patterns (Supplementary Fig. 4) exhibit a peak-like structure, with the second precipitation fraction on average the greatest in magnitude.

Figure 1 suggests that there is trend with latitude for the scaling. Figure 2a presents the results for each station from Fig. 1 along with the volume scaling (Supplementary Fig. 1) plotted against latitude. A smoothing spline has been fitted to the scaling, α. The scaling of the greatest precipitation fraction is generally positive and seems to increase slightly as the latitude trends further north. Conversely, the scaling of the smallest precipitation fraction is always negative and trends more negative for northerly latitudes. The scaling for the volume of the storm burst, although positive in the south of Australia, seems to decrease in the north of Australia. However, the positive scaling in the peak precipitation fraction is greater than the negative scaling in the overall burst volume, indicating a positive scaling in the peak precipitation intensity. Similar results, although smaller in magnitude, were obtained for a 30-min storm burst duration (Supplementary Fig. 12).

This analysis was repeated for storm durations of 120, 180, 360 and 720 min (Fig. 2b). For each duration considered, the temporal pattern consisted of five equal periods. In southern Australia, there was little change in the scaling between storm durations. There seems to be an almost constant value of scaling for the storm volume as well as for the first and fifth rank precipitation fractions. The storm volume and the first rank both scale positively, whereas the fifth rank scales negatively at a rate greater in magnitude than the increase in the storm volume.

In the north of Australia, the scaling of the volume with temperature is negative and decreases further as the storm duration increases. In fact the scaling is negative in the northern latitudes for storm durations longer than 120 min, suggesting a less intense storm. However, as the scaling of the first precipitation fraction is positive, with the magnitude of this scaling greater than the magnitude of negative volume scaling, a more intense storm is the result. The scaling of the fifth precipitation fraction decreases with latitude, indicating a less uniform temporal pattern with increased latitude. This trend is subdued when the analysis is repeated with dew point temperatures, suggesting humidity may be a limiting factor, especially in the tropics (Supplementary Figs 5 and 6).

It is apparent that the sensitivity of the storm temporal pattern dominates sensitivities in the overall storm burst intensity, especially in the tropics, where a negative scaling in the overall storm intensity is observed. Although generally an increase in volume will increase the flood discharge, increasing

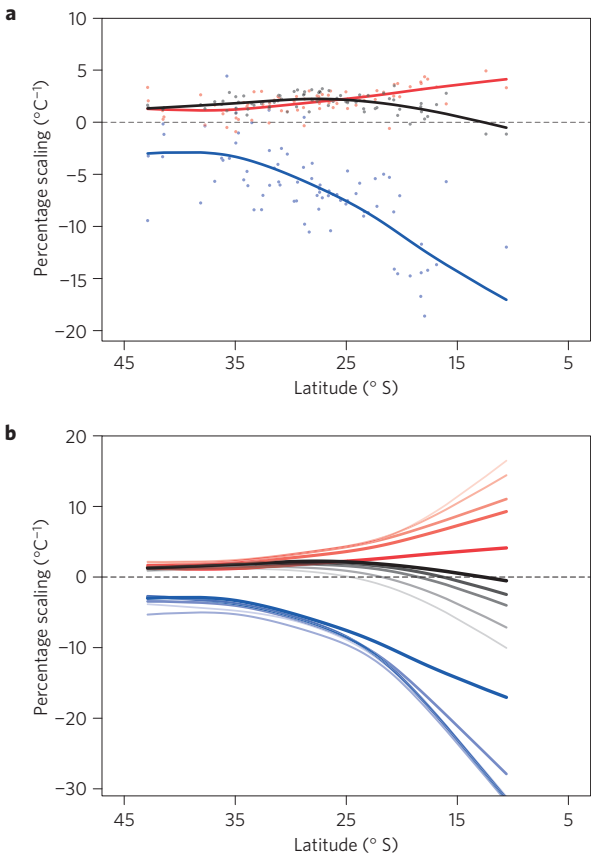

Figure 2 | Scaling of volume, first precipitation fraction, and last precipitation fraction, plotted against station latitude. a, Results for a 60-min storm burst duration. **b**, Result for varying storm burst duration. The thick lines are smoothing splines fitted to the measured scaling at the stations of interest. The lines in order of decreasing thickness and increasing transparency are for storm bursts of 60, 120, 180, 360 and 720 min, each with five equal periods. Scaling of volume (α_V) is in black, first precipitation fraction (α_1) in red, and last precipitation fraction (α_5) in blue.

non-uniformity of temporal patterns can also increase flooding, particularly for short durations (Supplementary Fig. 2). In general, applying the above temporal pattern scaling for a 5 °C rise resulted in 5–20% increases in the flood peak being modelled (Supplementary Table 2). Even at Darwin, where the overall storm volume scales negatively with temperature, an increase in the flood peak resulted from the increased non-uniformity of the temporal pattern.

It is generally assumed that as temperatures increase, as a response to a changing climate, the intensity of precipitation events may change in proportion to temperature changes. By investigating the scaling of temporal patterns within individual storm bursts, a consistent positive scaling for the highest precipitation fraction and a consistent negative scaling for the lowest precipitation fraction were found. This change in scaling is likely to be a combination of both the change in within-storm dependence as well as the impact of changed precipitation distributions at higher temperatures. Through randomization of the sample data, it was found that higher temperature precipitation exhibits a temporal dependence that significantly affects the temporal pattern structure compared to lower temperature precipitation.

Temporal patterns were found to be less uniform at higher temperatures—irrespective of the climatic region, precipitation type, or season—and a visual inspection of the temporal patterns confirmed this. Assuming sensitivities in the present climate are indicative of possible changes in a future climate, these results demonstrate, in addition to increased storm volumes, the possibility of invigoration of cloud motions with future warmer temperatures, which may result in less uniform and more destructive storms.

Methods

Methods and any associated references are available in the online version of the paper.

Received 23 March 2015; accepted 1 May 2015; published online 8 June 2015

References

1. Haerter, J. O. & Berg, P. Unexpected rise in extreme precipitation caused by a shift in rain type? *Nature Geosci.* **2,** 372–373 (2009).
2. Berg, P., Moseley, C. & Haerter, J. O. Strong increase in convective precipitation in response to higher temperatures. *Nature Geosci.* **6,** 181–185 (2013).
3. Collins, M. *et al.* in *Climate Change 2013: The Physical Science Basis* (eds Stocker, T. *et al.*) 1029–1136 (IPCC, Cambridge Univ. Press, 2013).
4. Boucher, O. *et al.* in *Climate Change 2013: The Physical Science Basis* (eds Stocker, T. *et al.*) 571–657 (IPCC, Cambridge Univ. Press, 2013).
5. Lenderink, G. & van Meijgaard, E. Increase in hourly precipitation extremes beyond expectations from temperature changes. *Nature Geosci.* **1,** 511–514 (2008).
6. Kirtman, B. *et al.* in *Climate Change 2013: The Physical Science Basis* (eds Stocker, T. *et al.*) 953–1028 (IPCC, Cambridge Univ. Press, 2013).
7. Westra, S. *et al.* Future changes to the intensity and frequency of short-duration extreme rainfall. *Rev. Geophys.* **52,** 522–555 (2014).
8. Alexander, L. V. *et al.* Global observed changes in daily climate extremes of temperature and precipitation. *J. Geophys. Res.* **111,** D05109 (2006).
9. Westra, S., Alexander, L. & Zwiers, F. Global increasing trends in annual maximum daily precipitation. *J. Clim.* **26,** 3904–3918 (2013).
10. Hartmann, D. L. *et al.* in *Climate Change 2013: The Physical Science Basis* (eds Stocker, T. *et al.*) 159–254 (IPCC, Cambridge Univ. Press, 2013).
11. Trenberth, K. E., Dai, A., Rasmussen, R. M. & Parsons, D. B. The changing character of precipitation. *Bull. Am. Meteorol. Soc.* **84,** 1205–1217 (2003).
12. Hardwick-Jones, R., Westra, S. & Sharma, A. Observed relationships between extreme sub-daily precipitation, surface temperature, and relative humidity. *Geophys. Res. Lett.* **37,** L22805 (2010).
13. Utsumi, N., Seto, S., Kanae, S., Maeda, E. E. & Oki, T. Does higher surface temperature intensify extreme precipitation? *Geophys. Res. Lett.* **38,** L16708 (2011).
14. Wasko, C. & Sharma, A. Quantile regression for investigating scaling of extreme precipitation with temperature. *Wat. Resour. Res.* **50,** 3608–3614 (2014).
15. Moseley, C., Berg, P. & Haerter, J. O. Probing the precipitation life cycle by iterative rain cell tracking. *J. Geophys. Res.* **118,** 13361–13370 (2013).
16. Singleton, A. & Toumi, R. Super-Clausius–Clapeyron scaling of rainfall in a model squall line. *Q. J. R. Meteorol. Soc.* **139,** 334–339 (2013).
17. Loriaux, J. M., Lenderink, G., De Roode, S. R. & Siebesma, a. P. Understanding convective extreme precipitation scaling using observations and an entraining plume model. *J. Atmos. Sci.* **70,** 3641–3655 (2013).
18. Panthou, G., Mailhot, A., Laurence, E. & Talbot, G. Relationship between surface temperature and extreme rainfalls: A multi-timescale and event-based analysis. *J. Hydrometeorol.* **15,** 1999–2011 (2014).

Acknowledgements

The authors are grateful for funding support from the Australian Research Council and the Institution of Engineers Australia. The authors wish to thank the Australian Bureau of Meteorology for data provision and support and U. Lall for fruitful conversations.

Author contributions

C.W. and A.S. conceived the initial idea. C.W. performed the analysis. C.W. and A.S. contributed to the manuscript.

Additional information

Supplementary information is available in the online version of the paper. Reprints and permissions information is available online at www.nature.com/reprints. Correspondence and requests for materials should be addressed to A.S.

Competing financial interests

The authors declare no competing financial interests.

Methods

Measurements of sub-daily precipitation and dry-bulb temperature from the Australian Bureau of Meteorology weather station data set (http://www.bom.gov.au/climate/data/stations) were used to extract a series of high-intensity storm bursts. Precipitation is typically measured using a tipping bucket rain gauge which measures precipitation at 6-min intervals. The dry-bulb temperature is measured in a shaded enclosure approximately 1.2 m above the ground surface and varies in resolution from 3-hourly to twice daily. The data set has been used extensively in previous studies[12,14,19].

The Australian continent covers a large range of expected scaling of precipitation with temperature, with climatic zones generally varying with latitude. In the north, the climate is tropical (Darwin), with high summer dominant precipitation. As we move south, inland the climate is arid with little precipitation (Alice Springs), whereas coastal areas vary from subtropical, with winter dominant precipitation (Perth), to temperate (Adelaide and Sydney), with a slightly wetter winter. Further south the climate is cool, with uniform precipitation (Hobart).

The analysis was restricted to stations that had more than 25 years of precipitation and temperature data with less than 10% of these data missing. Overall, 79 stations throughout Australia were considered. For a given weather station and a given duration, the largest 500 storm bursts in volume were chosen. For example, we start with data measured every 6 min. To find the largest 1-h storm burst, we find the sequence of rainfall of length one hour which has the greatest total depth. Once the largest storm burst is chosen it is removed from the precipitation record and the next largest storm burst is chosen from the remaining data. This ensures that the storm bursts do not overlap. The resultant series is the same as the partial series of storm maxima used in the estimation of design temporal precipitation patterns[20,21].

Using this method of storm burst selection, storm bursts can be adjacent to one another in time. Sensitivity tests were carried out on event choice by choosing independent storm events separated by two hours of zero precipitation. The storm bursts are then chosen as the maximum precipitation burst of 1-h duration from each of the events. Results are presented in Supplementary Fig. 9 and are consistent with the results presented.

The 6-min precipitation record was accumulated to ensure storm bursts were exactly five periods in length. For example, if a 1-h storm burst was analysed, the precipitation was accumulated to a duration of 12 min so the storm burst consists of five increments of equal duration. Similarly, a 2-h storm burst split into five increments consisting of five 24-min increments, and a 3-h storm burst, five 36-min increments. Every storm burst was matched to its coincident temperature. The temperature was calculated as the average over a 24-h moving window centred on the storm burst. This measurement was calculated to negate the influence of any possible short-term temperature fluctuations due to the event itself. By choosing the largest 500 events, we are considering those heavy rainfall events that occur throughout the year. For example, for a 25-year precipitation and temperature record, the frequency of events is approximately two per month. As a partial series can be of any length, the analysis was repeated using the greatest 10% of these storms. Although some evidence was found for increased scaling magnitudes of the precipitation fractions with decreasing event frequency, these were within confidence limits.

To calculate the volume scaling with temperature, for each partial series of storm bursts, an exponential regression was fitted to the storm-burst–temperature pairs[12,13] by regressing the logarithm of volume V against temperature T. This regression resulted in the following relationship between the storm volumes V_T and $V_{T+\Delta T}$, separated by a difference in temperature ΔT:

$$V_{T+\Delta T} = V_T(1+\alpha_V)^{\Delta T}$$

where α_V is the rate at which the volume changes per degree of temperature. Temporal patterns were then constructed by dividing the storm burst by its volume. The individual proportions within the temporal pattern were ranked from largest to smallest. The scaling with temperature for the fraction of precipitation in each rank was determined by fitting the following relationship:

$$P^i_{T+\Delta T} = P^i_T(1+\alpha_i)^{\Delta T}$$

where α_i is the scaling of the proportion of precipitation for rank i of the temporal pattern and P^i_T denotes the ith rank precipitation fraction corresponding to temperature T. Scalings were considered statistically significant at the 95% level. The hypothesis test performed was a t-test on whether the slope of the regression line differed from zero under the null hypothesis that the slope is zero. Confidence limits were obtained under the same assumptions.

As using dry-bulb temperature can neglect the effect of changes in relative humidity with temperature rise, the analysis was repeated using dew point temperature, which is a measure of the atmospheric moisture[18,22]. Using storm burst durations of 60, 120 and 180 min, the scaling of the precipitation fractions for the first and fifth rank was recalculated (Supplementary Figs 5 and 6). The results were consistent with those presented for dry-bulb temperature, albeit with reduced scaling magnitudes.

Sensitivity testing was also performed to see if the scaling calculated was different for precipitation events that are largely convective versus those that are largely non-convective (for example stratiform). One-hour storm bursts were demarcated using a critical precipitation intensity at which events above this intensity can be deemed convective[23,24]. The critical precipitation intensity was calculated at each site using all the data available for the site of interest. The scaling for the first fraction is very similar for both convective and non-convective precipitation (Supplementary Fig. 8), suggesting that the temporal pattern scaling occurs regardless of the type of precipitation event. This result is supported by the fact that when independently chosen precipitation events were stratified on season (summer or winter), when it is known that different types of precipitation dominate[25], the scaling of the precipitation fractions remained similar (Supplementary Fig. 11).

Flow-routing relationships were used to investigate the impact to flood peak due to changes in the temporal pattern as a result of a temperature increase. Such relationships have been used extensively to study catchment dynamics[26,27]. The storage S in a hydrologic system is related to the system inflow I and outflow Q by[28]:

$$\frac{dS}{dt} = I - Q$$

where S, I and Q are functions of time (t). The storage of the system, S, can be assumed to be a nonlinear function of the outflow of the form[28,29]:

$$S = kQ^m$$

where m is a dimensionless exponent representing the nonlinearity of the system and k represents the response time of the system and has units of time.

Representative catchment response times and catchment areas were chosen on the basis of the following relationship[30]:

$$t_c = 0.76A^{0.38}$$

where t_c is the time of concentration (or catchment response time) in hours and A is the area in km^2. Response times of 1 h, 2 h and 4 h were chosen and correspond to catchment areas of 2, 12 and 80 km^2.

For each site listed in Table 1, storm burst durations of one, two, three, six and twelve hours were simulated for storage exponents $m = 0.6, 0.7, 0.8, 0.9, 1.0$. Values of k were chosen to represent catchment response times of 1, 2 and 4 h. The temporal pattern used corresponded to the design temporal pattern[21]. A rainfall depth corresponding a 1% annual exceedance probability (AEP) event was adopted for illustration purposes. Each storm burst temporal pattern was scaled by 1 °C temperature increases up to 5 °C. The precipitation fraction scalings applied are similar to those used in the derivation of Fig. 2, with the exception that the temporal pattern was split into ten equal periods to improve the resolution of the flow routing. Scalings were recalculated for each individual duration and applied to the temporal pattern. If after applying the scaling the temporal pattern did not sum to unity, it was scaled to ensure the overall storm volume remained unchanged for temperature increases.

References

19. Westra, S. & Sisson, S. A. Detection of non-stationarity in precipitation extremes using a max-stable process model. *J. Hydrol.* **406,** 119–128 (2011).
20. Kennedy, M., Turner, L., Canterford, R. & Pearce, H. *Temporal Distributions within Rainfall Bursts* (Hydrology Report Series 1, Bureau of Meteorology, 1991).
21. Pilgrim, D. *et al.* in *Australian Rainfall and Runoff—A Guide to Flood Estimation* Book 2, Section 2 (The Institution of Engineers, 1997).
22. Lenderink, G. & van Meijgaard, E. Linking increases in hourly precipitation extremes to atmospheric temperature and moisture changes. *Environ. Res. Lett.* **5,** 025208 (2010).
23. Tremblay, A. The stratiform and convective components of surface precipitation. *J. Atmos. Sci.* **62,** 1513–1528 (2005).
24. Ruiz-Leo, A.M., Hernández, E., Queralt, S. & Maqueda, G. Convective and stratiform precipitation trends in the Spanish Mediterranean coast. *Atmos. Res.* **119,** 46–55 (2013).
25. Berg, P. *et al.* Seasonal characteristics of the relationship between daily precipitation intensity and surface temperature. *J. Geophys. Res.* **114,** D18102 (2009).
26. Kirchner, J. W. Catchments as simple dynamical systems: Catchment characterization, rainfall-runoff modeling, and doing hydrology backward. *Wat. Resour. Res.* **45,** W02429 (2009).
27. Pan, M. & Wood, E. F. Inverse streamflow routing. *Hydrol. Earth Syst. Sci.* **17,** 4577–4588 (2013).
28. Chow, V., Maidment, D. & Mays, L. *Applied Hydrology* (McGraw-Hill, 1988).
29. Brutsaert, W. *Hydrology—An Introduction* (Cambridge Univ. Press, 2005).
30. Pilgrim, D. in *Australian Rainfall and Runoff—A Guide to Flood Estimation* Book 4, Section 1 (The Institution of Engineers, 1997).